High-performance solar-blind ultraviolet photodetector based on mixed-phase ZnMgO thin film

M. M. Fan, K. W. Liu, Z. Z. Zhang, B. H. Li, X. Chen, D. X. Zhao, C. X. Shan, and D. Z. Shen

Citation: Applied Physics Letters **105**, 011117 (2014); doi: 10.1063/1.4889914
View online: http://dx.doi.org/10.1063/1.4889914
View Table of Contents: http://scitation.aip.org/content/aip/journal/apl/105/1?ver=pdfcov
Published by the AIP Publishing

High-performance solar-blind ultraviolet photodetector based on mixed-phase ZnMgO thin film

M. M. Fan,[1,2] K. W. Liu,[2,a)] Z. Z. Zhang,[2] B. H. Li,[2] X. Chen,[2] D. X. Zhao,[2] C. X. Shan,[2] and D. Z. Shen[2,a)]

[1]*Graduate University of the Chinese Academy of Sciences, Beijing 100049, People's Republic of China*
[2]*State Key Laboratory of Luminescence and Applications, Changchun Institute of Optics, Fine Mechanics and Physics, Chinese Academy of Sciences, No. 3888 Dongnanhu Road, 130033 Changchun, People's Republic of China*

(Received 28 April 2014; accepted 29 June 2014; published online 9 July 2014)

High Mg content mixed-phase $Zn_{0.38}Mg_{0.62}O$ was deposited on *a*-face sapphire by plasma-assisted molecular beam epitaxy, based on which a metal-semiconductor-metal solar-blind ultraviolet (UV) photodetector was fabricated. The dark current is only 0.25 pA at 5 V, which is much lower than that of the reported mixed-phase ZnMgO photodetectors. More interestingly, different from the other mixed-phase ZnMgO photodetectors containing two photoresponse bands, this device shows only one response peak and its −3 dB cut-off wavelength is around 275 nm. At 10 V, the peak responsivity is as high as 1.664 A/W at 260 nm, corresponding to an internal gain of ~8. The internal gain is mainly ascribed to the interface states at the grain boundaries acting as trapping centers of photogenerated holes. In view of the advantages of mixed-phase ZnMgO photodetectors over single-phase ZnMgO photodetectors, including easy fabrication, high responsivity, and low dark current, our findings are anticipated to pave a new way for the development of ZnMgO solar-blind UV photodetectors. © *2014 AIP Publishing LLC*. [http://dx.doi.org/10.1063/1.4889914]

Owing to the low natural background in the solar-blind ultraviolet (UV) region (<280 nm), photodetectors operating in this spectral range allow for a number of unique applications, including missile plume sensing, flame detection, chemical-biological agent sensing, and covert space-to-space communication.[1,2] The advantages in wide-band-gap (WBG) semiconductors, such as high radiation hardness and intrinsic visible/solar blind, have opened the possibility of developing high-performance WBG solar-blind UV photodetectors, which are recognized as the potential alternative for the photomultiplier tube and Si-based solar-blind UV photodetector.[3] Among WBG solar-blind UV photodetectors, ZnMgO-based devices have received the special attention due to their good material properties: low defect density, easy fabrication, and environmental friendly.[4–6] Till now, ZnMgO-based solar-blind UV photodetectors have been fabricated using different methods, such as metal organic chemical vapor deposition (MOCVD), RF-sputtering, and molecular beam epitaxy (MBE).[6–13] Most of these devices are based on the cubic ZnMgO (c-ZMO) due to their band gaps can be easily controlled in solar-blind region without any phase separation. However, c-ZMO-based devices usually show weak response to the light with wavelength below 280 nm.[7,10–12] In contrast to the c-ZMO, the wurtzite ZnMgO (w-ZMO) with the band gap in the solar-blind region is usually fabricated on ZnO substrate or buffer layer with a slow growth rate, and thus the realization of w-ZMO solar-blind photodetectors is still a big challenge.[8,9,13,14] Moreover, most of the solar-blind UV photodetectors based on w-ZMO usually have a small responsivity, which is similar to that of the c-ZMO-based devices.[9,13,14] Therefore, ZnMgO solar-blind photodetector with high responsivity is urgently demanded. Recently, it is demonstrated that the photodetectors fabricated on mixed-phase ZnMgO (m-ZMO) exhibit a relatively higher responsivity than that of the single-phase devices.[10,11,15] According to the previous reports, the interface states at the grain boundaries may play a key role in achieving this high responsivity.[16] Therefore, the high-responsivity solar-blind photodetectors are expected to be realized on the m-ZMO. However, the m-ZMO usually has two absorption edges: one is shorter than 280 nm and another one is longer than 300 nm, indicating that they are not suitable for solar-blind detection without external filters.[10,11,15,17] The lower Mg content of w-ZMO in mixed-phase alloys should be responsible for the longer absorption edge. Therefore, to realize the high-performance solar-blind photodetectors based on m-ZMO, the relatively high Mg content in w-ZMO is required.[8,9,13,14] However, no information can be found about it till now.

In this Letter, the m-ZMO with high Mg content has been fabricated by plasma-assisted MBE, and the photodetector based on these materials shows an extremely low dark current (5 V, 0.28 pA) with the −3 dB cut-off wavelength of 275 nm. Meanwhile, the responsivity at 260 nm can reach as high as 1.664 A/W at 10 V bias. The responsivity as a function of bias voltage and the dependence of photoresponse on different gas atmosphere at room temperature were analyzed to discuss the origin of high responsivity in our mixed-phase device.

The m-ZMO thin films were deposited on the *a*-face sapphire substrate by plasma-assisted MBE. 6N-purity zinc and 5N-purity magnesium held in thermal Knudsen cells and 5N-purity O_2 activated in a radio frequency plasma source were employed as precursors. During deposition, the substrate temperature was fixed at 450 °C, and the chamber

a)Authors to whom correspondence should be addressed. Electronic addresses: liukw@ciomp.ac.cn and shendz@ciomp.ac.cn

pressure was set at 10^{-3} Pa. The surface morphology and the thickness of the film were measured by scanning electron microscope (SEM) (HITACHI S-4800). Energy dispersive x-ray spectroscopy (EDS) (GENESIS 2000 XMS60S) measurement was carried out to study the composition of ZnMgO films. The structural properties were investigated by D/max-RA X-ray diffraction (XRD) (Rigaku) with Cu Kα as the radiation source ($\lambda = 0.154$ nm). The transmission and absorption spectra were recorded by a UV-3101PC scanning spectrophotometer.

Au (~30 nm thick) metal-semiconductor-metal (MSM) electrodes were deposited by a sputtering method at room temperature. 8 pairs of interdigital electrode structures with 10 μm width, 10 μm gap, and 300 μm length, were realized by photolithography and lift off technique. The current-voltage (*I-V*) properties and spectral responses of the fabricated devices were measured using semiconductor parameter analyzer (Keithely 2200) and 200 W UV-enhanced Xe lamp with a monochromator, respectively.

Fig. 1(a) shows the XRD pattern of the as-deposited ZnMgO and ZnO thin films (used as the control sample). The diffraction peaks at 35.12° and 36.70° can be assigned to the (002) orientation of w-ZMO and (111) orientation of c-ZMO, respectively. This result indicates that our sample is m-ZMO. Notably, a large (002) peak shift of w-ZMO toward the big angel side is clearly observed compared with that of ZnO, which is associated with replacing Zn atoms by Mg atoms as well as lattice stress effects.[18] In Fig. 1(b), the EDS result indicates that the composition of m-ZMO is $Zn_{0.38}Mg_{0.62}O$. In addition, surface morphology of m-ZMO with thickness of about 350 nm was scanned by SEM [see Fig. 1(c)]. Fig. 1(d) shows the transmission and absorption spectra of m-ZMO. It is clear that the sample has more than 85% average transmission in the visible region and has a very smooth absorption edge instead of two distinct features.[19] Moreover, the major absorption occurring in the wavelength shorter than 280 nm suggests that m-ZMO seems suitable for solar-blind detection. This result indicates that w-ZMO in our mixed-phase film should have relative higher Mg content, which is consist with the large (002) peak shift of w-ZMO in XRD pattern. According to the previous reports on w-ZMO with the band gap above 4.5 eV, the (002) diffraction peak is usually at about 34.9°–35.1°, and the Mg mole content is around 0.46–0.59.[8,13,14,20] Therefore, based on the XRD and transmission/absorption results in Figs. 1(a) and 1(d), we deduce that the Mg content and the band gap energy of w-ZMO in our mixed-phase alloys should be around 0.59 and 4.6 eV, respectively. The relatively high Mg content in w-ZMO can be understood like this: the lattice mismatch between ZnO and *a*-face sapphire substrate (less than 0.08%) is much smaller than that between ZnO and *c*-face sapphire (18.3% after 30° in-plane rotation), which is helpful for keeping wurtzite structure.[14,21] Using the similar method, we estimate the Mg content in c-ZMO is around 0.64 and the corresponding band gap energy should be ~5 eV.[12,18] Here, it must be mentioned that the above estimation is very rough.

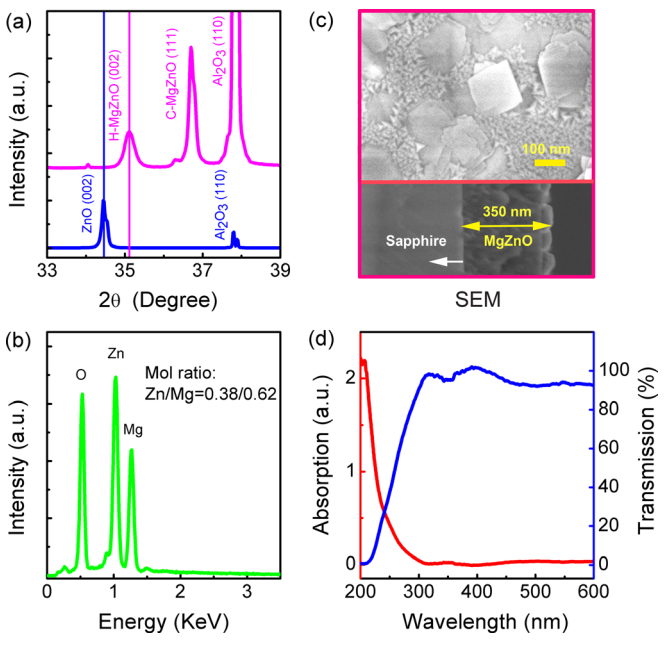

FIG. 1. (a) XRD spectra of m-ZMO and ZnO. (b) EDS spectrum, (c) SEM images, and (d) Transmission and absorption spectra of m-ZMO.

As shown in Fig. 2(a), the *I-V* characteristic of the m-ZMO photodetector was measured in a dark condition. The inset of Fig. 2(a) reveals the schematic illustration of MSM photodetector. It has 8 pairs of interdigital Au electrodes with 10 μm width, 10 μm gap, and 300 μm length (not to scale). The device exhibited a dark current as low as 0.25 pA at 5 V and 8.29 pA at 40 V, which is much lower than that of the reported m-ZMO photodetectors (see Table I). Considering that our device is based on m-ZMO, the inherently high resistance of c-ZMO should be responsible for the low dark current.[6,22] Moreover, according to the previous reports, with the increase of Mg content in w-ZMO, the net electron concentration decreases due to the strong carrier compensation effect, which thus results in a large resistance increasing.[23,24] Therefore, the high Mg content in w-ZMO should be another main reason for the low dark current in our mixed-phase device.

Figure 2(b) is the photoresponse spectrum of the m-ZMO photodetector at 10 V bias, and the inset shows the plot at logarithmic scales. The peak response occurs at 260 nm with the responsivity of 1.664 A/W and the corresponding internal gain (assuming quantum efficiency is unity) is 8. The −3 dB cutoff edge is around 275 nm, indicating our device is a true solar-blind photodetectors. In addition, the UV/visible rejection ratio defined as the ratio of responsivity at 260 nm and 400 nm is more than 3 orders of magnitude. More interestingly, the response band in UVA, commonly observed in m-ZMO photodetectors,[10,11,15,17] did not occur in our device, which can be attributed to the higher Mg content of w-ZMO. In addition, a very weak response can be found at around 300 nm, which should be associated with the alloy fluctuation of ZnMgO as well as the defects. Figure 2(c) is the maximum responsivity as a function of bias voltage, and a linear relationship can be observed between 5 and 40 V, indicating no carrier mobility saturation or sweep-out effect up to 40 V. In Fig. 3(a), the decay of current was recorded in air. The decay time (defined as the time for the current to decay to 10% of the peak value) of the

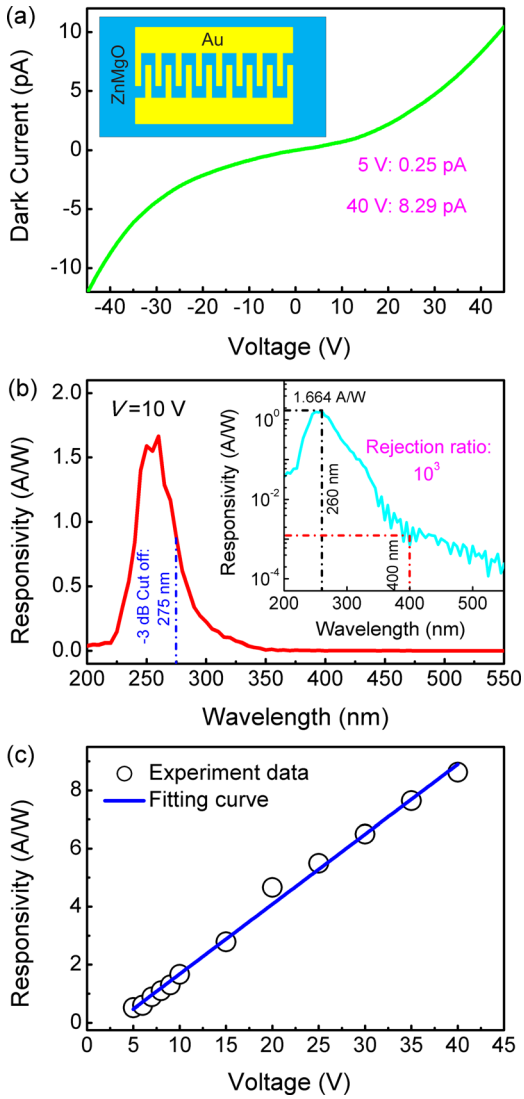

FIG. 2. (a) *I-V* characteristic of m-ZMO photodetector in dark. The inset is schematic illustration of MSM structure. (b) Spectral response of the photodetector at 10 V bias. The inset shows the spectral response in logarithmic scale. (c) Maximum responsivity as a function of bias.

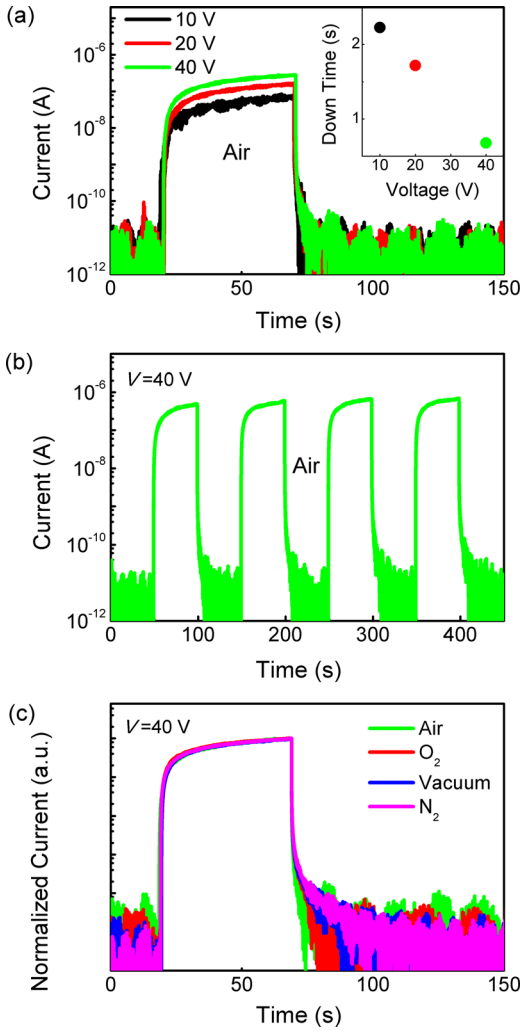

FIG. 3. Time-dependence photoresponse of m-ZMO photodetector under UV light illumination (260 nm). (a) UV photoresponse in air with different applied bias: 10 V (dark line), 20 V (red line), and 40 V (blue line). The inset shows the corresponding 90%-10% decay time. (b) Repeatable photoresponse at 40 V in air in logarithmic scale. (c) Normalized photoresponse in air (green line), O_2 (red line), vacuum (blue line), and N_2 (pink line) at 40 V in logarithmic scale.

device is about 1–2 s under different applied voltages. The reproducibility of the device was also tested by repeatedly switching UV light on and off for the same time intervals. In Fig. 3(b), the current of the device could be reversibly modulated by UV irradiation, indicating the good reproducibility and stability for the device. At 40 V, the peak responsivity can reach to 8.895 A/W and the corresponding internal gain is around 42. The origin of gain could be explained by the following part. According to the previous reports, it has been generally accepted that the presence of gain in ZnO-based

TABLE I. Dark current, peak responsivity, and cut-off wavelength of mixed-phase, wurtzite, and cubic ZnMgO photodetectors.

	Dark current	Peak responsivity	Cut-off wavelength	Growth method	Reference
m-ZMO	0.25 pA (5 V)	1.664 A/W (10 V)	275 nm	MBE	This work
	8.29 pA (40 V)	8.895 A/W (40 V)			
m-ZMO	...	60 A/W (1 V)	~275 nm; ~330 nm	MBE	10
m-ZMO	...	3 A/W (1 V)	~280 nm; ~350 nm	MBE	11
m-ZMO	...	462 A/W (1 V)	~275 nm; ~370 nm	MBE	15
m-ZMO	6 nA (3.5 V)	27 mA/W (−1.5 V)	~280 nm; ~400 nm	MOCVD	17
w-$Zn_{0.54}Mg_{0.46}O$	...	3.4 A/W (10 V)	~280 nm	Magnetron sputtering	8
w-$Zn_{0.45}Mg_{0.55}O$	1.4 pA (0.4 V)	22 mA/W (130 V)	270 nm	MBE	9
w-$Zn_{0.45}Mg_{0.55}O$	25 pA (150 V)	...	277 nm	MBE	13
c-$Zn_{0.46}Mg_{0.54}O$	0.45 pA (10 V)	396 mA/W (10 V)	265 nm	MOCVD	6
c-$Zn_{0.42}Mg_{0.58}O$	0.16 pA (15 V)	15.8 mA/W (15 V)	255 nm	MOCVD	22

MSM photodetectors is associated with the long life time of photogenerated holes.[8,25] This long life time is usually induced by the trap states of holes in the devices, such as the interface states between electrodes and semiconductor, the surface states, deep defects and grain boundaries in semiconductor and so on.[26–30]

The generation of interface states is usually inevitable at the interfaces of metal electrodes and material during the device processing. The trapping of photogenerated holes at the interface states could reduce the Schottky Barrier height and produce the internal gain, and the responsivity of these devices should obey a nonlinear relation with voltage.[26] However, the peak responsivity of our device exhibited a linear increase with the bias voltage up to 40 V as shown in Fig. 2(c). Therefore, the gain associated with the interface states between metal and semiconductor can be ruled out. Deep level defects in ZnMgO is another type of hole trapping states.[23,24,27] However, if the holes trapping at deep defect states is the dominate mechanism for the internal gain of our device, the solar-blind photodetectors based on high Mg content (above 50%) w-ZMO and c-ZMO should also have large responsivity. Conversely, the single-phase ZnMgO solar-blind photodetectors usually show weak response as shown in Table I. Therefore, the gain in this work is not derived from the deep defects in m-ZMO.

As is well known, the photoresponse of ZnO-based photodetectors is usually strongly affected by the absorption and desorption of gas molecules, especially oxygen molecules.[28,29] And the hole-trapping mechanism through oxygen adsorption and desorption in ZnO could enhance the photoresponse and can be responsible for the internal gain and slow recovery. In order to clarify this effect, time-dependent photoresponse measurement was carried out in different atmospheres (including N_2, O_2, air, and vacuum) under illumination of 260 nm UV light ($\sim$2.1 mW/cm^2). The normalized photoresponses shown in Fig. 3(c) reveals that the device shows the similar behavior in different atmospheres, and the decay time of the device is about 1 s in all cases. Therefore, the oxygen adsorption and desorption at the surface of ZnMgO are not the main reason for the internal gain and slow recovery in our device.

Considering the mixed-phase nature of our samples, the grain boundaries should be the most possible reason for the gain. According to the previous reports, the carrier trapping at grain boundaries could induce the energy barriers in m-ZMO, which impede the conduction of carriers between grains.[16] And this process is partly responsible for the low dark current of our device. Under UV light illumination, electron-hole pairs are created, and the photogenerated holes migrate to the grain boundaries and are subsequently captured. Thus, the excess life time of trapped holes should be the main reason for the internal gain and slow recovery.[30]

In conclusion, m-ZMO with high Mg content was realized on *a*-face sapphire by MBE. Owing to the high Mg content, both c- and w-ZMO have rather large band gaps ($E_g > 4.6$ eV). Therefore, our m-ZMO photodetector is a true solar-blind device with -3 dB cut-off wavelength of $\sim$275 nm. And the UV/visible rejection ratio is more than 3 orders of magnitude. Additionally, the dark current of our device is as low as 0.25 pA at 5 V, which is much lower than that of the reported m-ZMO photodetectors. The peak responsivity is 1.664 A/W at 10 V, corresponding to an internal gain of 8. The internal gain should be mainly contributed to the grain boundaries, which act as the trapping centers of photogenerated holes. The m-ZMO solar-blind photodetectors have clear advantages over the single-phase devices, including easy fabrication, high responsivity, and low dark current. Our findings are expected to pave a new way for the development of ZnMgO solar-blind UV photodetectors.

This work was supported by the National Basic Research Program of China (973 Program) (Nos. 2011CB302002 and 2011CB302006), the National Natural Science Foundation of China (Nos. 10974197, 11174273, 11104265, 11134009, and 61177040), the 100 Talents Program of the Chinese Academy of Sciences.

[1]T. Tut, M. Gokkavas, A. Inal, and E. Ozbay, Appl. Phys. Lett. **90**, 163506 (2007).
[2]E. V. Gorokhov, A. N. Magunov, V. S. Feshchenko, and A. A. Altukhov, Instrum. Exp. Tech. **51**, 280 (2008).
[3]E. Monroy, F. Omnes, and F. Calle, Semicond. Sci. Technol. **18**, R33 (2003).
[4]K. W. Liu, M. Sakurai, and M. Aono, Sensors **10**, 8604 (2010).
[5]Z. P. Zhang, H. von Wenckstern, and M. Grundmann, Appl. Phys. Lett. **103**, 171111 (2013).
[6]L. K. Wang, Z. G. Ju, J. Y. Zhang, J. Zheng, D. Z. Shen, B. Yao, D. X. Zhao, Z. Z. Zhang, B. H. Li, and C. X. Shan, Appl. Phys. Lett. **95**, 131113 (2009).
[7]Q. H. Zheng, F. Huang, J. Huang, Q. C. Hu, D. G. Chen, and K. Ding, CrystEngComm. **15**, 2709 (2013).
[8]Q. H. Zheng, F. Huang, J. Huang, Q. C. Hu, D. G. Chen, and K. Ding, IEEE Electron Device Lett. **33**, 1033 (2012).
[9]Y. N. Hou, Z. X. Mei, Z. L. Liu, T. C. Zhang, and X. L. Du, Appl. Phys. Lett. **98**, 103506 (2011).
[10]R. C. Boutwell, M. Wei, and W. V. Schoenfeld, Appl. Phys. Lett. **103**, 031114 (2013).
[11]R. C. Boutwell, M. Wei, and W. V. Schoenfeld, Appl. Surf. Sci. **284**, 254 (2013).
[12]Z. G. Ju, C. X. Shan, D. Y. Jiang, J. Y. Zhang, B. Yao, D. X. Zhao, D. Z. Shen, and X. W. Fan, Appl. Phys. Lett. **93**, 173505 (2008).
[13]X. L. Du, Z. X. Mei, Z. L. Liu, Y. Guo, T. C. Zhang, Y. N. Hou, Z. Zhang, Q. K. Xue, and A. Y. Kuznetsov, Adv. Mater. **21**, 4625 (2009).
[14]H. Endo, M. Kikuchi, M. Ashioi, Y. Kashiwaba, K. Hane, and Y. Kashiwaba, Appl. Phys. Express **1**, 051201 (2008).
[15]W. V. Schoenfeld, M. Wei, R. C. Boutwell, and H. Y. Liu, Proc. SPIE **8987**, 89871P (2014).
[16]I. Shalish, L. Kronik, G. Segal, Y. Shapira, S. Zamir, B. Meyler, and J. Salzman, Phys. Rev. B **61**, 15573 (2000).
[17]X. H. Xie, Z. Z. Zhang, C. X. Shan, H. Y. Chen, and D. Z. Shen, Appl. Phys. Lett. **101**, 081104 (2012).
[18]Z. Vashaei, T. Minegishi, H. Suzuki, T. Hanada, M. W. Cho, T. Yao, and A. Setiawan, J. Appl. Phys. **98**, 054911 (2005).
[19]Z. G. Ju, C. X. Shan, C. L. Yang, J. Y. Zhang, B. Yao, D. X. Zhao, D. Z. Shen, and X. W. Fan, Appl. Phys. Lett. **94**, 101902 (2009).
[20]T. Takagi, H. Tanaka, S. Fujita, and S. Fujita, Jpn. J. Appl. Phys., Part 1 **42**, L401 (2003).
[21]Ü. Özgür, Ya. I. Alivov, C. Liu, A. Teke, M. A. Reshchikov, S. Doğan, V. Avrutin, S.-J. Cho, and H. Morkoç, J. Appl. Phys. **98**, 041301 (2005).
[22]S. Han, J. Y. Zhang, Z. Z. Zhang, Y. M. Zhao, L. K. Wang, J. Zheng, B. Yao, D. X. Zhao, and D. Z. Shen, ACS Appl. Mater. Interfaces **2**, 1918 (2010).
[23]A. Hierro, G. Tabares, J. M. Ulloa, E. Muñoz, A. Nakamura, T. Hayashi, and J. Temmyo, Appl. Phys. Lett. **94**, 232101 (2009).
[24]M. Trunk, V. Venkatachalapathy, A. Galeckas, and A. Yu. Kuznetsov, Appl. Phys. Lett. **97**, 211901 (2010).

[25]L. Mandalapu, F. Xiu, Z. Yang, and J. Liu, Solid-State Electron. **51**, 1014 (2007).
[26]O. Katz, V. Garber, B. Meyler, G. Bahir, and J. Salzman, Appl. Phys. Lett. **79**, 1417 (2001).
[27]G. Tabares, A. Hierro, J. M. Ulloa, A. Guzman, E. Muñoz, A. Nakamura, T. Hayashi, and J. Temmyo, Appl. Phys. Lett. **96**, 101112 (2010).
[28]R. Ghosh and D. Basak, J. Appl. Phys. **101**, 113111 (2007).
[29]J. Lagowski, E. S. Sproles, Jr., and H. C. Gatos, J. Appl. Phys. **48**, 3566 (1977).
[30]M. A. Pietrzyk, E. Zielony, M. Stachowicz, A. Reszka, E. Płaczek-Popko, A. Wierzbicka, E. Przezdziecka, A. Droba, and A. Kozanecki, J. Alloys Compd. **587**, 724 (2014).